NEOPLASIA
www.neoplasia.com

Volume 10 Number 4 April 2008 pp. 329–339 329

Plasticity in Tumor-Promoting Inflammation: Impairment of Macrophage Recruitment Evokes a Compensatory Neutrophil Response[1,2]

Jessica C. Pahler*, Simon Tazzyman†, Neta Erez*, Yung-Yi Chen†, Craig Murdoch†, Hiroaki Nozawa*, Claire E. Lewis† and Douglas Hanahan*

*Department of Biochemistry and Biophysics, Comprehensive Cancer Center, and Diabetes Center, University of California – San Francisco, San Francisco, CA 94143, USA; †Tumor Targeting Group, Academic Unit of Pathology, The Henry Wellcome Laboratories for Medical Research, University of Sheffield Medical School, Sheffield S10 2RX, UK

Abstract

Previous studies in the K14-HPV/E_2 mouse model of cervical carcinogenesis demonstrated that infiltrating macrophages are the major source of matrix metalloproteinase 9 (MMP-9), a metalloprotease important for tumor angiogenesis and progression. We observed increased expression of the macrophage chemoattractant, CCL2, and its receptor, CCR2, concomitant with macrophage influx and MMP-9 expression. To study the role of CCL2-CCR2 signaling in cervical tumorigenesis, we generated CCR2-deficient K14-HPV/E_2 mice. Cervixes of CCR2-null mice contained significantly fewer macrophages. Surprisingly, there was only a modest delay in time to progression from dysplasia to carcinoma in the CCR2-deficient mice, and no difference in end-stage tumor incidence or burden. Moreover, there was an unexpected persistence of MMP-9 activity, associated with increased abundance of MMP-9^+ neutrophils in tumors from CCR2-null mice. *In vitro* bioassays revealed that macrophages produce soluble factor(s) that can suppress neutrophil dynamics, as evidenced by reduced chemotaxis in response to CXCL8, and impaired invasion into three-dimensional tumor masses grown *in vitro*. Our data suggest a mechanism whereby CCL2 attracts proangiogenic CCR2^+ macrophages with the ancillary capability to limit infiltration by neutrophils. If such tumor-promoting macrophages are suppressed, MMP-9^+ neutrophils are then recruited, providing alternative paracrine support for tumor angiogenesis and progression.

Neoplasia (2008) 10, 329–339

Introduction

Cervical cancer is the second most common form of malignancy among women worldwide [1]. The predominant risk factor for cervical cancer is the presence of oncogene-encoding DNA from the human papilloma virus types 16 and 18 (HPV16 and 18) and their *high-risk* papillomavirus relatives, which are found in 95% of all human cervical cancers [2]. A transgenic mouse model of this disease was developed by expressing the early region genes from HPV16 under the expression of the human keratin 14 promoter, restricting expression of the viral oncogenes to the basal squamous epithelium [3]. Female mice treated with sustained, low-dose estrogen (K14-HPV/E_2) synchronously develop cervical intraepithelial neoplastic (CIN) lesions that progress into cervical carcinomas, closely mimicking cervical cancer progression in humans [4]. Other characteristic markers of cervical *neoplasias*, such as increased blood vessel density, vascular endothelial growth factor production, and matrix metalloproteinase 9 (MMP-9) activity, parallel the human condition [5].

Previous studies have shown that high numbers of tumor-infiltrating macrophages (TIMs) correlate with poor prognosis in various forms of

Address all correspondence to: Douglas Hanahan, Diabetes Center HSW1090, 513 Parnassus Ave., Box 0534, San Francisco, CA 94143. E-mail: dh@biochem.ucsf.edu
[1]This work was supported by grants from the National Cancer Institute, USA (to D. H.) and by Yorkshire Cancer Research, UK (S. T., Y.Y. C., C. M., and C.E. L.). N. E. acknowledges a postdoctoral fellowship from the Irving Institute Fellowship Program of the Cancer Research Institute. The authors declare no competing financial interests.
[2]This article refers to supplementary material, which is designated by Figure W1 and is available online at www.neoplasia.com.
Received 19 September 2007; Revised 4 February 2008; Accepted 6 February 2008

DOI 10.1593/neo.07871

cancer, suggesting a role for these cells in tumor progression [6]. Furthermore, a number of studies have shown that TIMs express a broad range of tumor-promoting factors [7], and drive tumor angiogenesis and metastasis in a mouse mammary polyoma middle-T (MMTV-PyMT) tumor model [8,9]. In K14-HPV/E_2 mice, TIMs express abundant MMP-9, a protease known to promote tumor angiogenesis and growth [10].

Chemokines are a family of secreted proteins that induce cell survival and migration through specific G-coupled receptors [11]. CCL2 (MCP-1), acting through its only reported receptor, CCR2, induces the migration and activation of monocytes [12], and it has been implicated in the recruitment of TIMs and their expression of MMP-9 in several tumor types [13–16]. In human cervical cancer, CCL2 is abundantly expressed in the stroma and associated with macrophage infiltration [17]. Recent work by Zijlmans et al. [18] demonstrated that the absence of CCL2 mRNA expression in human cervical cancer specimens was associated with decreased macrophage infiltration and vascular invasion as well as smaller tumor size and increased overall survival. We therefore hypothesized that suppression of macrophage recruitment to the neoplastic cervix would lead to reduced MMP-9 expression, consequent inhibition of angiogenesis, and impaired tumor formation and growth.

Herein we report that CCL2 and CCR2 expression increases concordant with TIM-mediated inflammation during cervical carcinogenesis in the K14-HPV/E_2 model. However, when K14-HPV/E_2 mice were crossed with CCR2-null mice, the consequent reduction in TIM numbers failed to alter tumor angiogenesis or growth, but rather resulted in an increase in the number of tumor-infiltrating neutrophils expressing MMP-9. These data suggest that neutrophils can, in some circumstances, *compensate* for macrophage loss in tumors, serving to similarly facilitate tumor progression.

Materials and Methods

Transgenic Mice

The generation of K14-HPV [4] and CCR2-deficient mice [19] have been previously described. CCR2-null mice were backcrossed for six generations with FVB/n mice, then crossed with the K14-HPV mice to yield CCR2 heterozygous K14-HPV mice. These mice were then bred to yield CCR2-deficient K14-HPV mice. For these studies, 1-month-old CCR2-null, CCR2-heterozygous, and wild-type K14-HPV16 female mice were subcutaneously implanted with 60-day slow-release 17β-estradiol pellets (0.05 mg; Innovative Research, Sarasota, FL) at 1, 3, and 5 months of age (K14-HPV16/E_2) [20] and were maintained in accordance with the University of California, San Francisco (UCSF) institutional guidelines governing the care of laboratory mice.

Antibodies

The rabbit MMP-9 antibody was a kind gift from Dr. Z. Werb at UCSF [21]. The monoclonal rat anti–Meca-32, CD11b, and GR-1 were purchased from BD Biosciences (San Diego, CA). CD68 antibody was ordered from Serotec (Raleigh, NC) and F4/80 antibody and the PMN antibody, clone 7/4, were obtained from Cedarlane Laboratories (Ontario, Canada). The rabbit anti-CSF1R was from Chemicon (Waltham, MA), and the platelet-derived growth factor receptor (PDGFR) antibody was from eBioscience (San Diego, CA). Rabbit antimyeloperoxidase was purchased from DAKO (Cambridgeshire, UK). All secondary antibodies conjugated with either fluorescein isothiocyanate (FITC), Rhodamine-X, or biotin were purchased from Jackson ImmunoResearch (West Grove, PA).

Histology and Immunohistochemistry

Sections for both paraffin wax– and OCT-embedded frozen tumors were cut/prepared, and the antibody dilutions used were as follows: Meca-32 (diluted 1:200), F4/80 (diluted 1:100), CD68 (diluted 1:500), CD11b (diluted 1:100), CSF1R (1:200), PMN (diluted 1:500), GR-1 (1:50), and MMP-9 (diluted 1:400) and staining was carried out on frozen sections that had been blocked using 4% normal donkey serum in PBS. For 7/4 staining, sections were treated for 5 minutes with proteinase K (DAKO, Carpinteria, CA) before blocking. Tumor spheroid sections were incubated with anti–human myeloperoxidase for 30 minutes, otherwise all primary antibodies were incubated for 1 hour at room temperature followed by appropriate biotinylated or fluorescently conjugated secondary antibodies for 30 minutes at room temperature. Coverslips were then mounted on fluorescently labeled tissue using Vectamount with DAPI (Vector Laboratories). Fluorescent images were viewed with a 40×/0.75 air objective (except for blood vessels which were viewed with a 20×/0.50 air objective), collected using a microscope (AxioScope2 Plus; Zeiss, Thornwood, NY) with a digital camera (CA742-95; Hamamatsu, Bridgewater, NJ) and OpenLab software version 3.1.7 (Improvision, Lexington, MA). Biotinylated antibodies were developed with the standard elite ABC kit (Vector Laboratories, Burlingame, CA) with fast DAB (3′3′ diaminobenzidine tetrahydrochloride) (Sigma-Aldrich, St. Louis, MO). Slides were then counterstained with 1% methyl green and were dehydrated in isobutanol and 100% xylene before coverslips were mounted in a mounting medium (Cytoseal 60; Fisher Scientific, Pittsburgh, PA). Colorimetric images were acquired using Axioimager. A1 bright field microscope, AxioCam MRc5, and Axiovision AC version 4.3 (Zeiss) and were viewed through a 10×/0.45 or 40×/0.95 air objective. Magnifications were further increased using Adobe Photoshop version 7.0. Tissues were stained with secondary antibodies as controls, and background staining was minimal unless otherwise noted.

Tumor Evaluation

The characterization of tumor stages (based on hematoxylin and eosin staining) was performed as previously reported [22].

FACS Analysis

Cell sorting was carried out as previously published [23], using biotinylated- PDGFRα (eBioscience) with phycoerythrin-conjugated avidin (BD Biosciences) and FITC-conjugated F4/80 and CD68 antibodies (Serotec).

Real-Time Quantitative Polymerase Chain Reaction Analysis

RNA was isolated from samples using the RNeasy Kit (Qiagen, Valencia, CA) according to the manufacturer's directions. One microgram of RNA was denatured and primed at 65°C for 5 minutes with 3-μg random primers (Invitrogen, Carlsbad, CA) and then converted to cDNA using M-MLV reverse transcriptase (Promega, Madison, WI) in a final volume of 20 μl. For the sorted cell populations, the WT-Ovation RNA Amplification Kit (NuGen, San Carlos, CA) was used according to the manufacturer's directions to obtain at least 1 μg of cDNA for each sample. Real-time quantitative polymerase chain

reaction analysis (qRT-PCR) was carried out at the UCSF cancer genomics core using commercially available probes for CCL2 and CCR2 from Applied Biosystems (Foster City, CA).

Substrate Zymography

Tissues were processed and analyzed as previously described [24]. All cervical samples were isolated from 4-month-old K14-HPV/E_2 or CCR2-null K14-HPV/E_2 mice. At least five samples were analyzed per genotype. Ear tissue was isolated from 6-month-old K14-HPV mice as a positive control. Recombinant MMP-9 was purchased from Chemicon (Temecula, CA).

Monocyte Isolation

Human buffy coats were obtained from the National Blood Transfusion Service in the UK. This was diluted 1 in 5 calcium and magnesium-free Hanks's balanced salt solution (HBSS), and 10-ml aliquots were added to 250 μl of RosetteSep (Stem Cell, London, UK) solution and incubated for 20 minutes. Twenty milliliters of HBSS 2% FCS was added to the blood mixture that was then overlaid onto Ficoil-Paque Plus (Amersham Biosciences, Uppsala, Sweden) and centrifuged at 1200*g* for 20 minutes. The monocyte layer was collected, washed twice, and labeled with CellTracker blue (Molecular Probes, Paisley, UK), before coculturing with spheroids. Flow cytometry showed that <95% of these were $CD14^+$ monocytes.

Neutrophil Isolation

Human peripheral blood from healthy volunteers was treated with an anticoagulant, 3.8% w/v sodium citrate solution (BDH/AnalaR, Poole, UK), and then centrifuged at 400*g* for 20 minutes; the upper serum layer was then removed. The remaining cells were diluted 50:50 with HBSS (BioWhittaker, Berk, UK), overlaid onto Ficoll-Paque Plus (Amersham Biosciences), and centrifuged at 400*g* for 40 minutes. The neutrophil/erythrocyte layer was collected and subjected to hypertonic lysis to remove erythrocytes. The remaining neutrophils were washed and routinely found to be more than 95% viable.

In Vitro *Neutrophil Migration Assay*

Human monocytes or the human breast tumor cell line, T47D, cells were seeded at 30,000 cells/well in 100 μl of Dulbecco's modified Eagle's medium containing 1% FCS in a 96-well plate for 4 hours and washed; adherent cells were then incubated for 24 hours (the control medium was incubated for the same period without either cell type). Supernatants were then collected, sterile-filtered, supplemented with or without 10 nM CXCL8, and added to the lower wells of a 48-well microchemotaxis chamber. A polycarbonate membrane with 3-μm pores was placed on top of the chamber and 50 μl of 1×10^6 neutrophils/ml in Dulbecco's modified Eagle's medium containing 1% FCS was added to the upper wells for 1 hour at 37°C. The number of neutrophils in the lower chamber was then quantified by flow cytometry using CellQuest software (BD Biosciences, San Jose, CA).

Monocyte/neutrophil Infiltration Into Tumor Spheroids

Human tumor spheroids were generated by seeding 5000 human tumor (HeLa cervical cancer) cells in 100 μl of culture medium in each well of an agarose-coated 96-well plate and were incubated at 37°C, 5% CO_2 for 7 to 8 days. Before infiltration with leukocytes, spheroids were cultured overnight in a 96-well plate with Minimal Essential Medium with Earl's salts (MEME), to stimulate intercellular adhesion molecule 1 expression (and thus facilitate monocyte/neutrophil adhesion and infiltration). Either 6×10^5 neutrophils/ml (prelabeled with cell tracker red) or monocytes (prelabeled with cell tracker blue) in serum-free MEME were added to each well and left for 5 (neutrophils) or 24 hours (monocytes) at 37°C in a 5% CO_2 incubator. Spheroids were then removed, washed twice in serum-free MEME, and resuspended in 100 μl of serum-free MEME. Spheroids infiltrated with monocytes were cultured for a further 5 hours with the same concentration of freshly isolated neutrophils (again labeled red), whereas spheroids infiltrated with neutrophils were cocultured with freshly isolated monocytes (labeled blue) for a further 24 hours. A shorter period was used for neutrophil cocultures than those involving monocyte as they are known to be more labile in culture than monocytes. Spheroids were then trypsinized in 0.25% trypsin for 5 to 10 minutes at 37°C, washed, and analyzed by flow cytometry to estimate the proportion of neutrophils, monocytes, and/or tumor cells. In parallel cultures, spheroids were fixed with 10% buffered formalin for 1 hour and were then embedded in a solution of molten 1.5% agarose and 4% formaldehyde (BDH/Merck, Poole, UK), machine-processed (TP1020; Leica, Wetzler, Germany), and embedded in paraffin wax. Neutrophils and/or monocytes were identified in sections of tumor spheroids by staining for myeloperoxidase.

Statistical Analysis

F4/80, CD68, CSF1R, PMN, and MMP-9 expressions were determined by counting the staining per field using a custom Adobe Photoshop Plug-in. At least five fields from each slide (mouse) were measured with at least four mice for each group and an average/field determined. These averages, as well as tumor volume, were compared by nonparametric analysis of variance using InStat Software (GraphPad, San Diego, CA). A chi-square analysis was used to evaluate tumor incidence. In the cell migration assays, differences between treatments groups were analyzed using the nonparametric Mann-Whitney U test.

Results

CCL2 and CCR2 Are Upregulated in the K14-HPV/E_2 Mouse Model of Cervical Carcinoma

To assess the expression of CCL2 ligand and CCR2 receptor during cervical carcinogenesis, real-time quantitative RT-PCR analysis was performed on cervical tissues from normal (FVB/n) and dysplastic (3 months old) K14-HPV/E_2 mice. CCL2 expression was prominently upregulated at this time point (i.e., 2 months after carcinogenesis was initiated with sustained estrogen), when macrophage infiltration of CIN 1/2 lesions becomes prevalent (Figure 1*A*). Likewise, CCR2 exhibited increased expression at this early stage of neoplastic progression concomitant with macrophage recruitment into tumors (Figure 1*B*). In an effort to determine which population of cells was producing the ligand and receptor, cell sorting was performed. A single cell suspension from 3-month-old cervixes was sorted into $PDGF\alpha^+F4/80^-CD68^-$ (fibroblasts), $F4/80^+CD68^+$ macrophages, and other unstained cells (a mixed-cell population of epithelial cells, other inflammatory cells, and endothelial cells). The RNA from these populations was amplified, and qRT-PCR was used to analyze CCL2 expression. Both the fibroblast and mixed-cell populations expressed CCL2 at

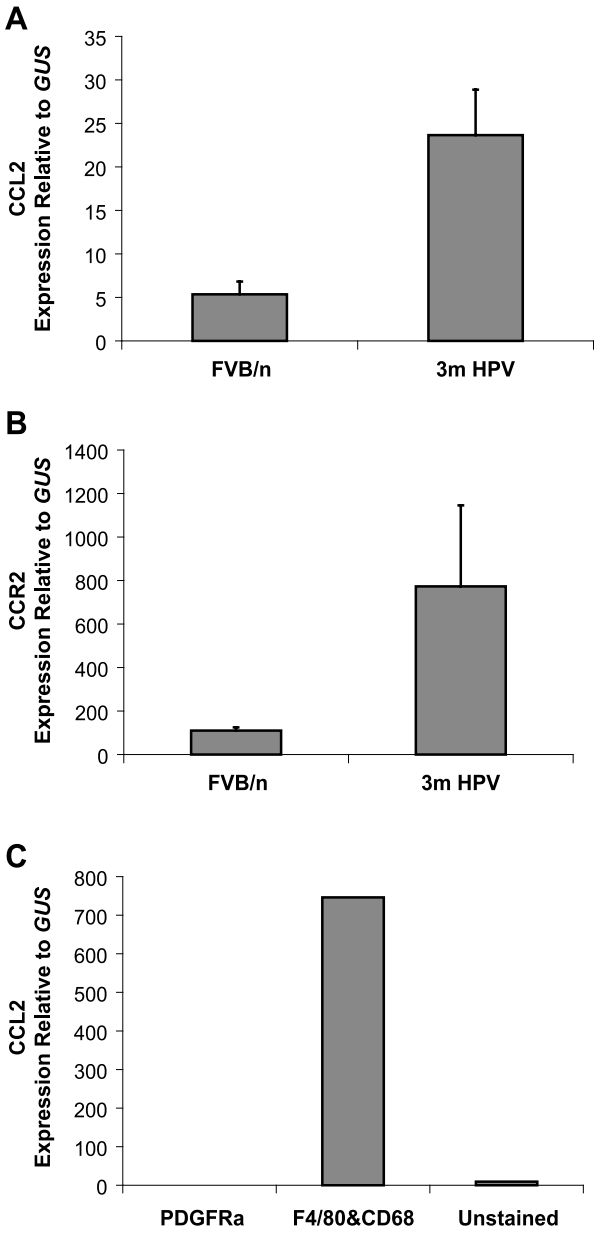

Figure 1. CCL2 and CCR2 are upregulated during K14-HPV/E_2 tumorigenesis. RNA was isolated from the cervix of three estrogen-treated nontransgenic FVB/n, and K14-HPV mice with dysplasia (3 months) and real-time quantitative PCR used to determine (A) CCL2 and (B) CCR2 expression. Additionally, RNA was isolated from sorted fibroblasts (PDGFRα$^+$), myeloid cells (F4/80$^+$ and/or CD68$^+$), and the remaining unstained cells from a pool of 10 cervixes from 3-month-old mice and qRT-PCR used to measure CCL2 expression in these populations (C). CCL2 expression was 0.07 in the PDGFRα$^+$ population. Expression levels were normalized to those of the housekeeping gene *GUS*. Error bars show SEM.

low/negligible levels compared to macrophages. CCR2, as expected, was predominantly expressed by the F4/80$^+$CD68$^+$ population in tumors (data not shown).

Effect of CCR2 Deficiency on Tumor Progression

CCR2-deficient mice, originally described by Boring et al. [19], were backcrossed into the FVB/n background for six generations and then crossed with the K14-HPV16 transgenic mice to produce CCR2-null HPV16 mice. We first analyzed the temporal appearance and progression of neoplastic lesions in HPV16/E_2 female mice that lacked CCR2. Surprisingly, neither was there a difference in the timing or histologic character of the progressive CIN 1, 2, and 3 lesions (data not shown) nor was there a difference in the incidence, tumor burden, or histologic characteristics of cervical carcinomas (Figure 2*A*, and data not shown). There was, however, a modest, albeit statistically significant, delay in the timing of malignant progression. Overt cervical carcinomas were detected in 60% of CCR2$^{+/+}$ and CCR2$^{+/-}$ HPV16/E_2 mice at 4 months, whereas there were no tumors detected in the CCR2$^{-/-}$ cohort at this time point. However, neoplastic lesions emerged in the CCR2$^{-/-}$ mice a few weeks later, and after an additional month, the incidence in all three cohorts was 100% (Figure 2*B*).

We next analyzed the angiogenic phenotype, motivated both by our previous demonstration that MMP-9 expressing macrophages were instrumental in promoting new blood vessel growth, and by previous studies, particularly in hypoxic environments, that had

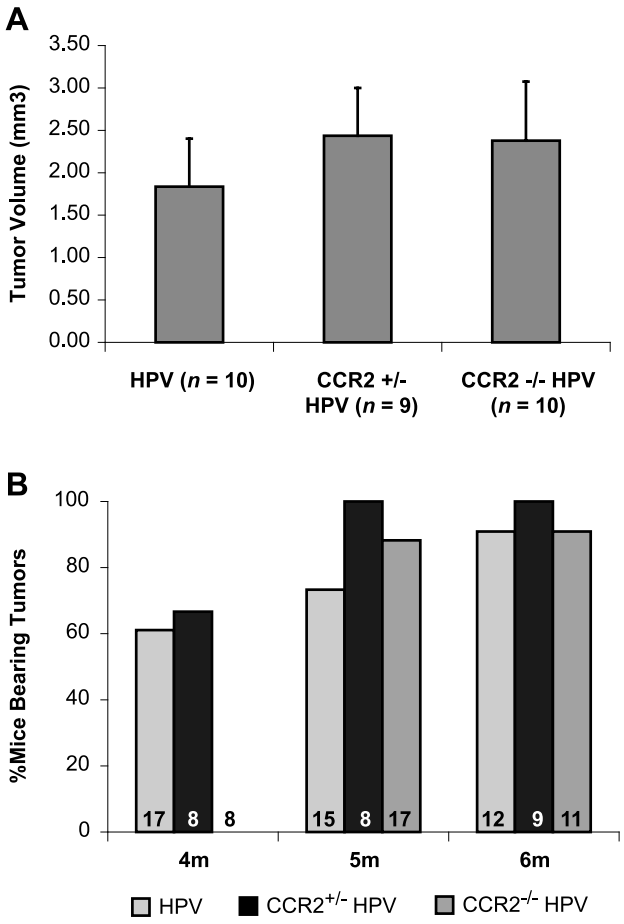

Figure 2. Absence of CCR2 delays time-to-tumor onset but does not affect tumor growth or incidence. Tumor incidence and burden were assessed using hematoxylin and eosin–stained serial sections using tissue collected from mice at 4 months, between 4.25 and 5 months, and more than 5 months of age. (A) Tumor volume (growth) was not significantly different between any genotype at end stage. (B) Tumor incidence was significantly delayed ($P < .001$) at the earliest stages in CCR2-null K14-HPV/E_2 mice. The *n* values for each group are displayed at the base of each bar.

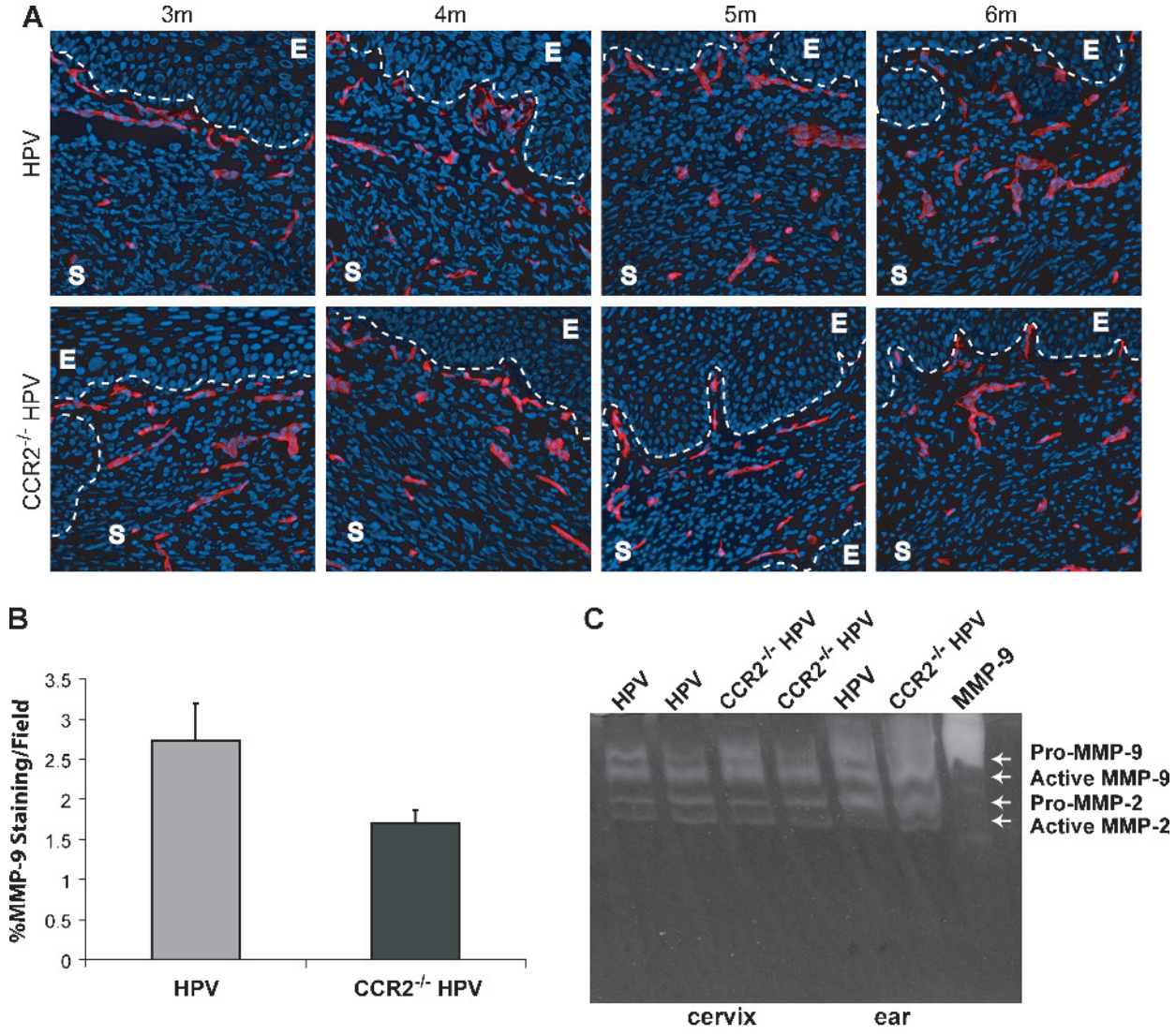

Figure 3. Effect of CCR2 deficiency on tumor angiogenesis and MMP-9 expression. (A) Immunohistochemical analysis of Meca-32 (Rhodamine, red; endothelial cells) in tumor sections at 1-month intervals during tumorigenesis revealed no striking differences. E indicates the epithelium; S, stroma. Nuclei are shown in blue by staining with DAPI; original magnification, ×200. (B) Tissue sections were immunohistochemically stained with an antibody against MMP-9, and expression per field was quantified in the cervical stroma of 4-month-old K14-HPV/E_2 and CCR2-null K14-HPV/E_2 mice (P = .03). (C) Tissues were collected from mice at the same age, and nonquantitative substrate zymography was performed to assess the presence of MMP activity.

directly implicated CCL2 in inducing angiogenesis [25]. Blood vessel morphology and density were assessed using immunofluorescence for two markers, Meca-32 (Figure 3*A*) and CD31 (data not shown). Comparative evaluation of cervical tissue from 3-, 4-, 5-, and 6-month-old CCR2-null and wild-type K14-HPV/E_2 mice revealed no appreciable difference in either vessel parameter (data not shown). Immunohistochemistry for MMP-9 was also performed on tumor sections from 4-month old mice, which revealed only a small decrease in expression in CCR2-deficient mice (Figure 3*B*). Because MMP-9 is synthesized as a precursor molecule that must be cleaved to be activated, expression does not always indicate activity. Therefore, nonquantitative gelatin zymography was used to assess MMP-9 activity at the same time point. Figure 3*C* demonstrates that there were comparable levels of active MMP-9 protease in the cervix of both wild-type and CCR2-deficient K14-HPV/E_2 mice. Dysplastic skin from these mice, which were shown to have elaborate MMP-9 activity [26], again showed little impact of CCR2 deficiency on the levels of active protease. The above results indicate that a sufficient level of MMP-9 is being produced in the CCR2 knock-out mice to support tumor angiogenesis and tumor progression. We therefore sought to assess the effect of CCR2 deficiency on the abundance of TIMs in this model, because one explanation of our data would be that TIM infiltration persisted in the absence of CCR2 deficiency.

CCR2 Deficiency Diminishes Macrophage Recruitment and Activation

Because macrophage infiltration of the neoplastic lesions in the cervix is prominent at 4 months of age in K14-HPV/E_2 mice, this time point was used to analyze macrophage recruitment in the absence of CCR2. Tissue sections were stained with antibodies against F4/80 (a marker for mature macrophages) and CD68 (which labels

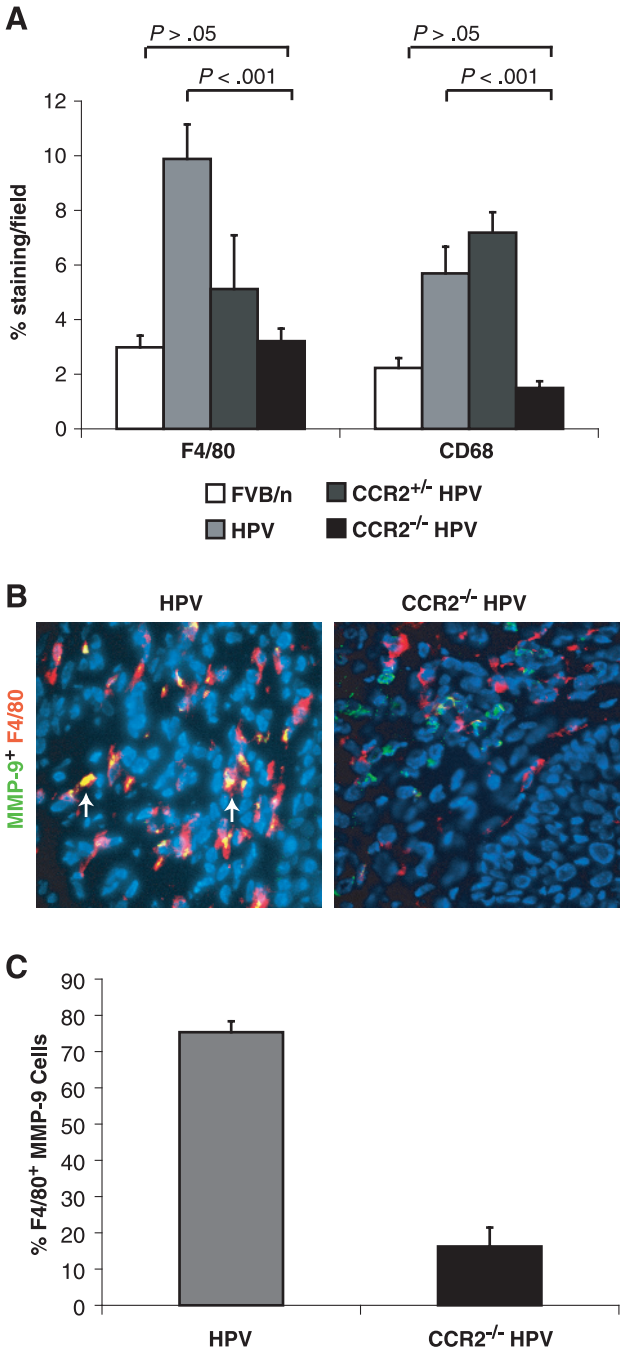

Figure 4. CCR2 inhibition blocks macrophage recruitment to the cervical stroma. (A) Immunohistochemical analysis of F4/80 and CD68 was performed, and staining was quantified per field in nontransgenic FVB/n and 4-month-old CCR2 wild-type, heterozygous, and null K14-HPV/E_2 mice. In all cases, there are significantly fewer positively stained cells in the CCR2-null mice compared to wild-type K14-HPV/E_2 mice. There is no significant difference in expression between nontransgenic and CCR2-deficient transgenic mice. (B) Images of MMP-9 (FITC, green) colocalization with the macrophage marker F4/80 (Rhodamine, red) in 4-month-old wild-type and CCR2-null K14-HPV/E_2 mice. Yellow indicates colocalization, and green arrows indicate MMP-9^+, F4/80^- cells. Original magnification, ×400. (C) % of all MMP-9 cells expressing F4/80.

all monocytes/macrophages). Cervical intraepithelial neoplastic lesions in K14-HPV/E_2 mice were infiltrated with higher numbers of macrophages than those in CCR2-null K14-HPV/E_2 mice (Figure 4*A*). The density of stained cells in the CCR2-deficient mice was comparable to estrogen-treated nontransgenic mice (FVB/n/E_2), suggesting that only resident macrophages rather than inflammatory macrophages were present (Figure 4*A*). Because CCL2 signaling has been implicated in the synthesis and activation of MMP-9 in monocytes [13], MMP-9 expression was also analyzed in these *resident* macrophages. Notably, marked changes in expression patterns were evident. In wild-type mice, MMP-9 was expressed almost exclusively by F4/80^+ macrophages, whereas in the CCR2-null mice, the frequency of MMP-9 coexpression with F4/80 was markedly reduced (Figure 4, *B* and *C*). This difference suggested that an alternative cell type might be supplying the comparable levels of MMP-9 detected in the CCR2-null K14-HPV/E_2 mice.

Neutrophils Are Abundant in the Tumor Stroma of CCR2-Null K14/HPV/E_2 Mice

Tumor-infiltrating neutrophils have been reported to express MMP-9 in another mouse model of cancer, the RIP-Tag2 islet carcinoma model [27]. Therefore, immunofluorescent analysis was carried out using the monoclonal antibody clone 7/4, which recognizes a cell surface antigen present on neutrophils (as well as a subset of monocytes). Costaining of MMP-9 with 7/4 revealed that 7/4^+ cells in CCR2-null K14-HPV/E_2 mice expressed MMP-9, whereas they failed to do so in tumors in wild-type mice (Figure 5*A*).

The presence of MMP-9^+ neutrophils in the macrophage-depleted tumors of CCR2 deficient mice suggested a possible compensatory mechanism in which MMP-9 is supplied by a different inflammatory cell population. This hypothesis warranted further analysis. Because the 7/4 monoclonal antibody is reported to label macrophages in addition to neutrophils [28], immunohistochemical staining with 7/4 was carried out in conjunction with hematoxylin and eosin staining to assess the cell morphology of 7/4^+ cells in tumors in wild-type and CCR2-null K14-HPV/E_2 mice. Many of the 7/4^+ cells in wild-type lesions were identifiable as macrophages, as judged by their size and the round appearance of their nuclei. In contrast, the 7/4^+ cell population in tumors of CCR2-null K14-HPV/E_2 mice had the typical multilobed nucleus indicative of neutrophils (Figure 5*B*). Costaining of these populations using an antibody for CSF1R (another marker of cells of the monocyte/macrophage lineage) showed colocalization in the majority of 7/4^+ cells in the CCR2^+ wild-type mouse, confirming that these were, indeed, macrophages. Conversely, staining in tumors in CCR2-null mice showed no expression of CSF1R by 7/4^+ cells (Figure 5*B*). Quantitative analysis of the staining of these two populations in tumors revealed that 7/4^+, CSF1R^+ macrophages were abundant in wild-type, but rare in the CCR2-deficient K14-HPV/E_2 mice, whereas 7/4^+, CSF1R^- neutrophils were prevalent in CCR2-null and rare in the CCR2 wild-type K14-HPV/E_2 mice (Figure 5*C*).

We went on to further analyze the 7/4^+ populations in both the wild-type and CCR2-null mice. As expected, costaining with CD68 showed staining similar to CSF1R (Figure 6). Costaining with the mature macrophage marker, F4/80, showed no colocalization with 7/4 in either tumor genotypes (Figure 6), indicating that the 7/4^+, CSF1R^+ population consists of monocytes and/or relatively immature macrophages. GR-1, a neutrophil marker, was coexpressed with 7/4 in tumors in CCR2-deficient mice, whereas minimal coexpression was detected in the cervix of wild-type HPV mice (Figure 6). Finally, CD11b/

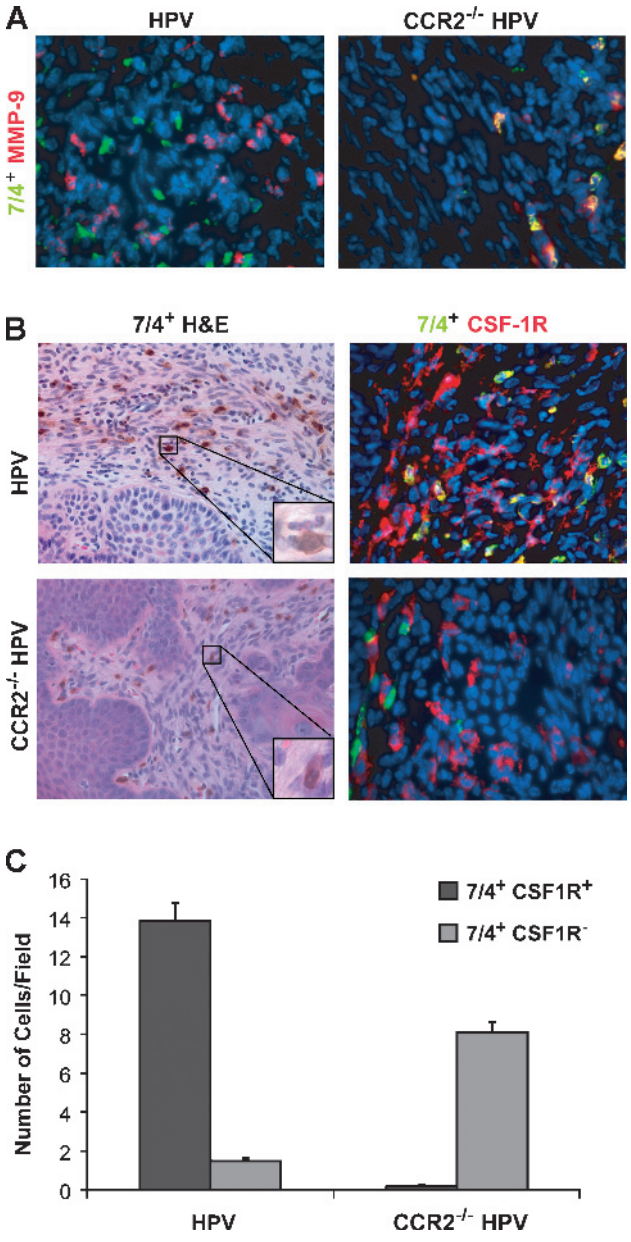

Figure 5. Neutrophil expression colocalizes with MMP-9 in CCR2-deficient mice. Immunohistochemistry was performed with MMP-9 and the neutrophil antibody clone 7/4 on tissues from 4-month-old mice. (A) Representative images of MMP-9 (Rhodamine, red) colocalization with the 7/4 clone (FITC, green) in wild-type and CCR2-null K14-HPV/E_2 cervical tissues. (B) Hematoxylin and eosin staining (original magnifications: ×100 for large panel and ×1000 for inset) with the 7/4 clone shows that 7/4 is expressed on macrophages in K14-HPV/E_2 mice and on neutrophils in the CCR2-null counterparts. Neutrophils can be clearly identified by morphology in the null mice but were rare in the cervical stroma of wild-type mice. 7/4 staining (FITC, green) of macrophages was further confirmed by colocalization with the macrophage marker CSF1R (Rhodamine, red) only in wild-type mice. Original magnification, ×400 for all fluorescent images. (C) Staining for both 7/4 single-positive and 7/4 and CSF1R double-positive populations was determined in both mouse genotypes ($P < .001$).

Mac-1, which is expressed at varying levels by neutrophils, monocytes, macrophages, and other inflammatory cells, was expressed on all $7/4^+$ cells in the null mice. Notably, CD11b is upregulated on activated neutrophils. However, CD11b was expressed on only a portion of the $7/4^+$ cells in wild-type CCR2 cervical *neoplasias*, emphasizing the heterogeneity of this myeloid population (Figure 6).

Collectively, these data suggest an inflammatory leukocyte infiltrate in the neoplastic cervix of wild-type mice composed of immature macrophages ($7/4^+$, $CSF1R^+$, $F4/80^-$, $MMP\text{-}9^-$), activated inflammatory macrophages ($7/4^-$, $CSF1R^+$, $F4/80^+$, $MMP\text{-}9^+$), along with mature and/or resident macrophages ($7/4^-$, $CSF1R^+$, $F4/80^+$, $MMP\text{-}9^-$), with neutrophils being relatively rare. In contrast, the cervical *neoplasias* in CCR2-deficient mice have abundant neutrophils ($7/4^+$, $GR\text{-}1^+$, $CSF1R^-$, $F4/80^-$, $MMP\text{-}9^+$), along with similar levels of resident macrophages, but with comparatively few immature and inflammatory macrophages.

Macrophages Inhibit Neutrophil Recruitment

We investigated two mechanisms by which the abundance of neutrophils in tumors in CCR2-null mice might be explained. One was that, in the absence of macrophages, cervical tumors upregulate neutrophil chemoattractants and/or survival factors, thus importing a new source of MMP-9. Another was that signals emanating from TIMs in wild-type mice normally block neutrophil recruitment and/or survival, and that these inhibitory signals were therefore missing in tumors in CCR2-deficient HPV/E_2 mice.

In an effort to assess the first possibility, we audited a set of cytokines and chemokines associated with neutrophil recruitment by qRT-PCR of 4-month-old wild-type and CCR2-deficient cervical tissue. There was no appreciable change in expression of CCL3, CCL5, CXCL1, CXCL2, G-CSF, and IL-23 (data not shown). Only one gene, *GM-CSF*, demonstrated upregulation of mRNA that would be consistent with increased neutrophil inflammation in the CCR2-null tissues; there was, however, no difference in GM-CSF expression at the protein level as assessed by immunostaining (data not shown). Thus, this survey did not implicate increased expression of neutrophil chemoattractants as the basis for the neutrophil inflammation of cervical *neoplasias* in CCR2-null mice.

To investigate the alternative hypothesis that infiltrating macrophages normally prevent neutrophil recruitment and/or inhibit their survival, we employed two *ex vivo* cell migration assays. First, we used a modified Boyden chamber chemotaxis assay to examine the effect of monocyte-derived factors on neutrophil migration in response to the well-characterized neutrophil chemoattractant, CXCL8. Medium alone, medium containing recombinant human CXCL8, or medium conditioned previously by human monocytes or another cell type (in this case, the human tumor cell line, T47D) was placed in the lower chamber of the assay device, with or without the addition of CXCL8. Neutrophils isolated from human peripheral blood were then placed in the upper chamber, separated from the lower one by a 3-μm-pore membrane. After 1 hour, the number of neutrophils that had migrated to the lower chamber was counted. CXCL8 induced a significant ($P = .01$) increase in the number of neutrophils migrating across the filter into the lower chamber. This CXCL8-dependent chemotaxis was ablated by the addition of medium conditioned by monocytes but not tumor cells with or without added CXCL8 (Figure 7*A*), indicating that monocytes produce one or more soluble factors that inhibit neutrophil migration in response to CXCL8.

To better emulate events occurring within the tumor microenvironment, we also used a tumor spheroid model described by us previously [29], in which tumor cells seeded in nonadherent culture dishes grow as spherical, three-dimensional tumor masses. Tumor spheroids have previously been observed to elicit infiltration of both monocytes and neutrophils by virtue of their release of various chemokines (including CCL2) [29]. Two human tumor cell lines, HeLa, derived from a cervical carcinoma, which expresses the HPV-18 oncogenes, and A549, a lung carcinoma–derived cell line, were cultured for 7 to 8 days under conditions that allow tumor spheroids of 700 to 800 μm in diameter to develop. These spheroids were then preincubated overnight with $CD14^+$ monocytes freshly isolated from human peripheral blood, which resulted in the marked infiltration of monocytes into the spheroids. Then the monocyte-infiltrated spheroids were incubated for 5 hours with peripheral blood neutrophils. Spheroids were then enzymatically dispersed, the cells collected for flow cytometry, and the number of spheroid-infiltrating neutrophils determined. There was a significant ($P < .01$) decrease in the number of neutrophils present in spheroids following preincubation with monocytes with both types of tumor cell spheroids (Figure 7*B*). Immunohistochemistry for the enzyme myeloperoxidase, illustrating the infiltration of neutrophils into tumor spheroids, is shown in Figure 7*C*. Tumor spheroids derived from both lines showed the same ability to separately recruit monocytes or neutrophils, indicating that the sequential addition of macrophages followed by neutrophils resulted in an active restriction of neutrophil infiltration that would otherwise occur.

Taken together, the two cell culture experiments indicate that monocytes produce one or more factors that inhibit neutrophil infiltration into tumors. To determine if neutrophils could similarly inhibit macrophage recruitment, the same spheroid experiment was carried out in the opposite order, using both human tumor cell lines. Spheroids were preincubated with neutrophils for 5 hours, during which time they infiltrated the spheroids, followed by an overnight incubation with monocytes. Subsequent flow cytometric analysis revealed no difference in the number of infiltrated monocytes, suggesting that preexisting neutrophils are not able to inhibit monocyte chemotaxis under these conditions (Figure W1).

Discussion

This study has investigated the hypothesis that macrophage inflammation of cervical *neoplasias* and cancers is mediated by signaling of the CCL2-CCR2 chemokine circuit. Whereas the results show, as expected, a reduced number of macrophages, there was an unexpected persistence of MMP-9 levels in the tumors of mice, a surprising result in light of clear evidence that TIMs are the major source of this enzyme in cervical *neoplasias* in this model as well as in humans [9,30]. Seeking an explanation for this dichotomy, we discovered an alternative source of MMP-9 – neutrophils – in tumors in CCR2-null mice. Seeking in turn to explain this increased infiltration of $MMP\text{-}9^+$ neutrophils, we assessed the expression of neutrophil chemoattractants and survival factors, finding no obvious difference between wild-type and CCR2-deficient tumors. In contrast, two *ex vivo* bioassays involving human macrophages and neutrophils revealed that macrophages were capable of suppressing neutrophil chemotaxis and infiltration, but not vice versa, potentially providing a rationale for the distinctive inflammatory cell dynamics in cervical lesions of the CCR2-positive *versus* CCR2-null genotypes. These observations, involving two distinctive human tumor-derived cell lines, are certainly suggestive rather that definitive, but nevertheless encourage the hypothesis that the capability of monocytes to inhibit neutrophil infiltration may be operative in multiple tumor types, including cervical carcinoma and lung.

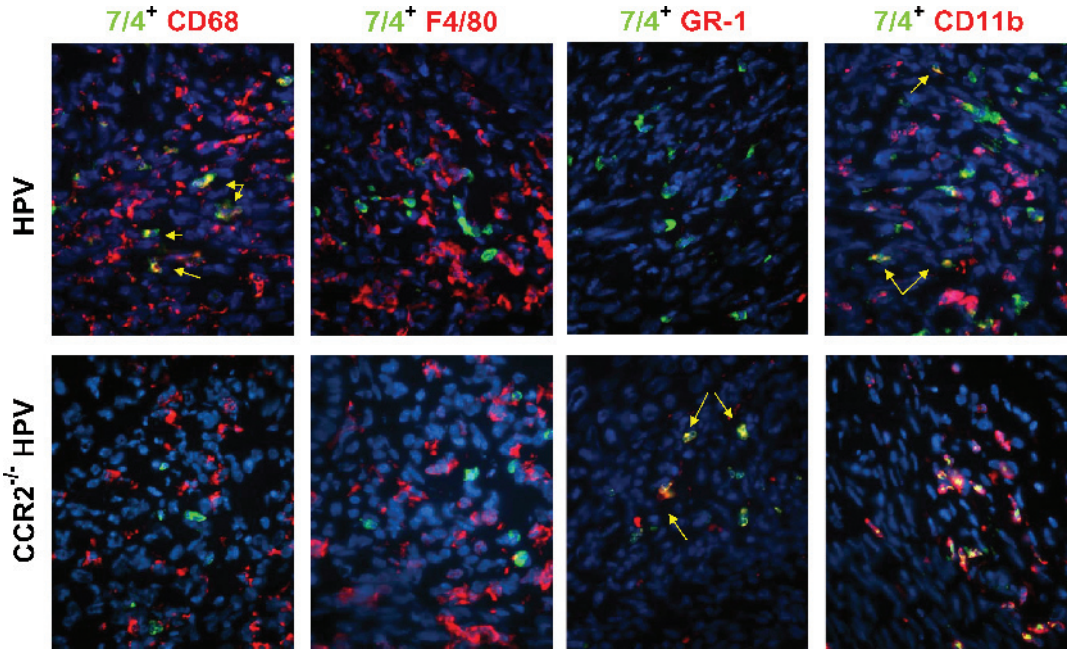

Figure 6. Colocalization of $7/4^+$ cells with macrophage and neutrophil markers in the cervix. Tissue sections from both wild-type and CCR2-deficient mice were stained with antibodies against CD11b, GR-1, CD68, and F4/80 (Rhodamine, red) and with the 7/4 clone (FITC, green) to further characterize these cells as having neutrophil markers in CCR2-null mice and macrophage markers in wild-type mice. Yellow arrows indicate coexpression. Original magnification, ×400.

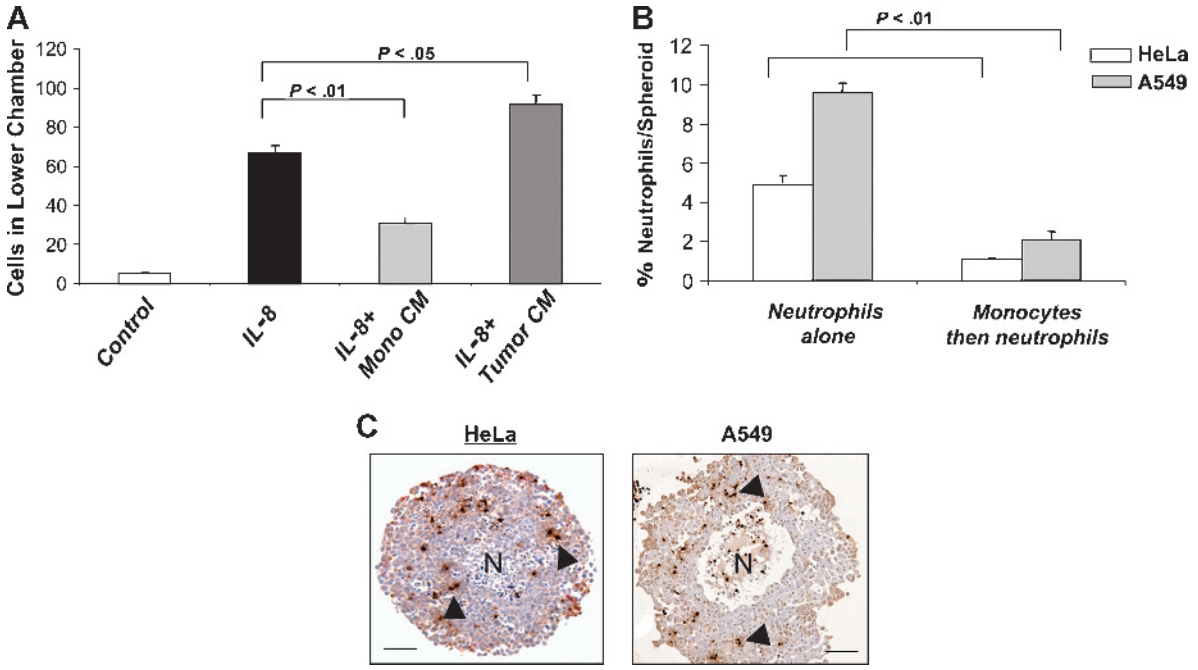

Figure 7. Monocytes inhibit neutrophil migration and infiltration into human tumor spheroids *in vitro*. (A) Cell migration assays were carried out using control, monocyte-conditioned medium (CM), or tumor cell CM spiked with the neutrophil chemoattractant CXCL8 as described in Materials and Methods. CXCL8 promoted neutrophil migration that was significantly ablated in the presence of monocyte CM but not of tumor cell CM. (B) Human tumor (cervical; HeLa or lung; A549) spheroids were cocultured with either neutrophils alone for 5 hours or monocytes for 16 hours followed by neutrophils for 5 hours. Spheroids were then washed and enzymatically digested, and flow cytometry was used to quantify the number of infiltrating neutrophils. Significantly ($P < .001$) fewer neutrophils infiltrated into spheroids when monocytes were already present in these structures than when they were absent. (C) Immunohistochemistry using an antimyeloperoxidase antibody (brown; arrows) illustrates the presence of neutrophils in tumor spheroids following coculture. This marker could detect both monocytes and neutrophils in HeLa spheroids when the latter were cocultured with each cell type alone. However, there was no (cumulative) increase in MPO^+ cell number when monocytes were allowed to infiltrate spheroids before their culture with neutrophils (data not shown). N indicates the necrotic core at the center of spheroids. Scale bar, 150 μm.

As previously mentioned, we were not able to identify changes in chemokines associated with neutrophil recruitment. Instead, our *in vitro* bioassays suggest an alternative explanation: in some tumor types, macrophages can suppress neutrophil migration and/or persistence by their release of one or more soluble factor(s). Infiltrating neutrophils are typically short-lived inside tissues (usually lasting only a few hours), and thus accumulation of macrophages could quickly block ongoing neutrophil chemotaxis and encourage the resolution of neutrophil inflammation. It has also been proposed that macrophages influence neutrophil accumulation during inflammation through phagocytosis of the apoptotic neutrophils [31], and may even induce apoptosis in neutrophils directly [32]. For instance, Li et al. [33] found that blocking CCL2 using a neutralizing antibody or a peptide antagonist of CCR2 resulted in a delayed clearance of apoptotic neutrophils in a rat model of tubulointerstitial nephritis. Although we did not detect an increase in neutrophil apoptosis in the stroma of tumors of CCR2-deficient mice (data not shown), given the rapid kinetics of apoptosis and the 6-month time-course of progression in this model, we were not able to rule out macrophage-induced neutrophil apoptosis as a factor in the differential abundance of neutrophils in wild-type *versus* CCR2-deficient cervical *neoplasias* and cancers.

A similar capability of macrophages to influence the dynamics of neutrophil infiltration and function has been implicated in other studies of inflammation in CCR2-null mice. One study reported persistent neutrophils in the peritoneum up to 5 days after intraperitoneal injection of the proinflammatory agent thioglycollate in CCR2-null but not wild-type mice [34]. In another study, granuloma formation following zymosan A injection was found to be attenuated in CCR2-null mice, with an atypical increase in neutrophils inside the granulomas [35]. CCR2-deficient mice infected with influenza virus were also found to have increased alveolar neutrophils [36].

Altered neutrophil regulation has also been observed in CSF-1 mutant mice; CSF-1 is a major growth factor in the development, proliferation, and survival of monocytes and macrophages [37]. CSF-1 mutant mice ($csf1^{op}/csf1^{op}$) are impaired in macrophage differentiation and inflammatory phenotypes, as seen both in the context of inflammation induced by bacterial infection [38] and mammary carcinogenesis [7,8]. Notably, a persistence of infiltrating neutrophils was observed in the livers of CSF-1 mutant mice following *Listeria monocytogenes* infection [38]. Neutrophils are abundant in the context of macrophage deficiency in the MMTV-PyMT, $csf1^{op}/csf1^{op}$ model of breast carcinogenesis (J.W. Pollard, personal communication). In this case, however, the malignant phenotype is impaired by the reduction in macrophage influx [39], indicating that neutrophils cannot fully substitute for the macrophage effector functions, which includes supply of epidermal growth factor [40] and vascular endothelial growth factor [8]. These differences highlight the potential for tissue-specific (and perhaps tumor type–specific) variations in tumor-promoting inflammatory responses. Indeed, there are indications of heterogeneity in cervical cancers, given that reduced CCR2

levels in one study correlated with a better prognosis [18]; whereas other undefined variables may influence this correlation, on inference is that neutrophil substitution was not pronounced or was ineffectual in this patient population, possibilities that deserve further investigation in other human population studies.

Additionally, other functional studies in mouse models and correlative/prognostic studies in human tumors have revealed complexity and, indeed, a dichotomy in the effects of infiltrating macrophages on tumor phenotypes. In many tumor types, macrophages promote angiogenesis, tumor growth, and metastasis, and their presence correlates with poor prognosis and survival [6]. In other tumor types, macrophages appear to inhibit such phenotypes, perhaps reflecting the effects of an antigen-presenting macrophage involved in antitumor immune responses. These conflicting correlations suggest the existence of distinct macrophage populations genetically determined early in monocyte differentiation and/or elicited by the local microenvironment. CCR2 expression, which has been attributed to inflammatory rather than resident macrophages [41], may characterize a predetermined set of macrophages that have proinflammatory and ultimately protumor properties. Whereas these cells are recruited to sites of inflammation through CCR2-CCL2 signaling, it seems likely that local factors in the neoplastic microenvironment instruct these cells to mediate tumor-promoting functions, including MMP-9 expression and activation.

The cervical microenvironment appears to reflect one class of organ-specific tumors, in which macrophages are selectively recruited during neoplastic development, much as in the aforementioned model of MMTV-PyMT breast cancer [8]. Another mouse model, of pancreatic islet carcinoma, is characterized by early infiltration of MMP-9–expressing neutrophils as well as two distinctive classes of MMP-9$^+$ and MMP-9$^-$ macrophage [26,27]. Thus, the neoplastic microenvironment clearly governs the dynamics of proangiogenic leukocyte infiltration. Notably, macrophage inflammation is mild in the pancreatic islet cancer model, in contrast to the cervix and breast tumor models, where the macrophage influx is more pronounced. It could be that a critical density of lesional macrophages is necessary to suppress the influx and persistence of neutrophils.

A related issue involves the source in the cervical *neoplasias* of the ligand for CCR2 that mediates macrophage recruitment. By using FACS and qRT-PCR, we determined that the CCL2-producing cells in the cervix are myeloid-derived cells recruited to the early neoplastic microenvironment of the cervix through a yet unknown mechanism, presumably a result of expressing the HPV oncogenes in the epithelium. The recruitment of these CCL2-expressing cells appears to be independent of CCR2, because there was no decrease in CCL2 expression in the cervix of CCR2-deficient HPV/E_2 mice (data not shown). The nature of these proinflammatory myeloid cells, and the mechanism by which they are recruited to in turn recruit CCR2$^+$ MMP-9$^+$ macrophages that promote angiogenesis and tumorigenesis, deserves future investigation.

In conclusion, this study has revealed a complex interplay between tumor-infiltrating macrophages and neutrophils that contributes to neoplastic progression. The plasticity of leukocyte inflammation revealed in this study, in which proangiogenic neutrophils replace the functions of proangiogenic macrophages when the latter are suppressed, has potential therapeutic implications. If the recruitment of proangiogenic macrophages into cervical tumors is blocked pharmacologically, neutrophils may replace them, thereby minimizing any therapeutic benefit. Thus, in considering clinical strategies targeting tumor-promoting macrophages, it may prove that efficacy will be determined in part by the capability of certain tissues (and/or tumor types) to affect resistance through substitution, involving infiltration of compensatory neutrophils in the context of macrophage suppression.

Acknowledgments

We thank I. Charo of UCSF for supplying the CCR2-null mice, C. Chiu for his critical reading of the manuscript, and E. Drori, S. Cacacho, M. Vayner, C. Guinto, and A. Wang for technical support.

References

[1] Waggoner SE (2003). Cervical cancer. *Lancet* **361**, 2217–2225.
[2] Bosch FX and de Sanjose S (2003). Chapter 1: Human papillomavirus and cervical cancer—burden and assessment of causality. *J Natl Cancer Inst Monogr* **31**, 3–13.
[3] Coussens LM, Hanahan D, and Arbeit JM (1996). Genetic predisposition and parameters of malignant progression in K14-HPV16 transgenic mice. *Am J Pathol* **149**, 1899–1917.
[4] Arbeit JM, Howley PM, and Hanahan D (1996). Chronic estrogen-induced cervical and vaginal squamous carcinogenesis in human papillomavirus type 16 transgenic mice. *Proc Natl Acad Sci USA* **93**, 2930–2935.
[5] Smith-McCune K, Zhu YH, Hanahan D, and Arbeit J (1997). Cross-species comparison of angiogenesis during the premalignant stages of squamous carcinogenesis in the human cervix and K14-HPV16 transgenic mice. *Cancer Res* **57**, 1294–1300.
[6] Bingle L, Brown NJ, and Lewis CE (2002). The role of tumour-associated macrophages in tumour progression: implications for new anticancer therapies. *J Pathol* **196**, 254–265.
[7] Lewis CE and Pollard JW (2006). Distinct role of macrophages in different tumor microenviroments. *Cancer Res* **66**, 605–612.
[8] Lin EY, Nguyen AV, Russell RG, and Pollard JW (2001). Colony-stimulating factor 1 promotes progression of mammary tumors to malignancy. *J Exp Med* **193**, 727–740.
[9] Lin EY, Li JF, Gnatovskiy L, Deng Y, Zhu L, Grzesik DA, Qian H, Xue XN, and Pollard JW (2006). Macrophages regulate the angiogenic switch in a mouse model of breast cancer. *Cancer Res* **66**, 11238–11246.
[10] Giraudo E, Inoue M, and Hanahan D (2004). An amino-bisphosphonate targets MMP-9–expressing macrophages and angiogenesis to impair cervical carcinogenesis. *J Clin Invest* **114**, 623–633.
[11] Balkwill F (2003). Chemokine biology in cancer. *Semin Immunol* **15**, 49–55.
[12] Audran R, Lesimple T, Delamaire M, Picot C, Van Damme J, and Toujas L (1996). Adhesion molecule expression and response to chemotactic agents of human monocyte-derived macrophages. *Clin Exp Immunol* **103**, 155–160.
[13] Robinson SC, Scott KA, and Balkwill FR (2002). Chemokine stimulation of monocyte matrix metalloproteinase-9 requires endogenous TNF-alpha. *Eur J Immunol* **32**, 404–412.
[14] Koide N, Nishio A, Sato T, Sugiyama A, and Miyagawa S (2004). Significance of macrophage chemoattractant protein-1 expression and macrophage infiltration in squamous cell carcinoma of the esophagus. *Am J Gastroenterol* **99**, 1667–1674.
[15] Ueno T, Toi M, Saji H, Muta M, Bando H, Kuroi K, Koike M, Inadera H, and Matsushima K (2000). Significance of macrophage chemoattractant protein-1 in macrophage recruitment, angiogenesis, and survival in human breast cancer. *Clin Cancer Res* **6**, 3282–3289.
[16] Amann B, Perabo FG, Wirger A, Hugenschmidt H, and Schultze-Seemann W (1998). Urinary levels of monocyte chemo-attractant protein-1 correlate with tumour stage and grade in patients with bladder cancer. *Br J Urol* **82**, 118–121.
[17] Kleine-Lowinski K, Gillitzer R, Kuhne-Heid R, and Rosl F (1999). Monocyte–chemo-attractant-protein-1 (MCP-1)-gene expression in cervical intra-epithelial *neoplasias* and cervical carcinomas. *Int J Cancer* **82**, 6–11.
[18] Zijlmans HJ, Fleuren GJ, Baelde HJ, Eilers PH, Kenter GG, and Gorter A (2006). The absence of CCL2 expression in cervical carcinoma is associated with increased survival and loss of heterozygosity at 17q11.2. *J Pathol* **208**, 507–517.
[19] Boring L, Gosling J, Chensue SW, Kunkel SL, Farese RV Jr, Broxmeyer HE, and Charo IF (1997). Impaired monocyte migration and reduced type 1 (Th_1) cytokine responses in C-C chemokine receptor 2 knockout mice. *J Clin Invest* **100**, 2552–2561.

[20] Elson DA, Riley RR, Lacey A, Thordarson G, Talamantes FJ, and Arbeit JM (2000). Sensitivity of the cervical transformation zone to estrogen-induced squamous carcinogenesis. *Cancer Res* **60**, 1267–1275.

[21] Behrendtsen O, Alexander CM, and Werb Z (1992). Metalloproteinases mediate extracellular matrix degradation by cells from mouse blastocyst outgrowths. *Development* **114**, 447–456.

[22] Riley RR, Duensing S, Brake T, Munger K, Lambert PF, and Arbeit JM (2003). Dissection of human papillomavirus E6 and E7 function in transgenic mouse models of cervical carcinogenesis. *Cancer Res* **63**, 4862–4871.

[23] Bergers G, Song S, Meyer-Morse N, Bergsland E, and Hanahan D (2003). Benefits of targeting both pericytes and endothelial cells in the tumor vasculature with kinase inhibitors. *J Clin Invest* **111**, 1287–1295.

[24] Coussens LM, Raymond WW, Bergers G, Laig-Webster M, Behrendtsen O, Werb Z, Caughey GH, and Hanahan D (1999). Inflammatory mast cells up-regulate angiogenesis during squamous epithelial carcinogenesis. *Genes Dev* **13**, 1382–1397.

[25] Weber KS, Nelson PJ, Grone HJ, and Weber C (1999). Expression of CCR2 by endothelial cells: implications for MCP-1 mediated wound injury repair and *in vivo* inflammatory activation of endothelium. *Arterioscler Thromb Vasc Biol* **19**, 2085–2093.

[26] Coussens LM, Tinkle CL, Hanahan D, and Werb Z (2000). MMP-9 supplied by bone marrow–derived cells contributes to skin carcinogenesis. *Cell* **103**, 481–490.

[27] Nozawa H, Chiu C, and Hanahan D (2006). Infiltrating neutrophils mediate the initial angiogenic switch in a mouse model of multistage carcinogenesis. *Proc Natl Acad Sci USA* **103**, 12493–12498.

[28] Henderson RB, Hobbs JA, Mathies M, and Hogg N (2003). Rapid recruitment of inflammatory monocytes is independent of neutrophil migration. *Blood* **102**, 328–335.

[29] Bingle L, Lewis CE, Corke KP, Reed MW, and Brown NJ (2006). Macrophages promote angiogenesis in human breast tumour spheroids *in vivo*. *Br J Cancer* **94**, 101–107.

[30] Davidson B, Goldberg I, Kopolovic J, Lerner-Geva L, Gotlieb WH, Weis B, Ben-Baruch G, and Reich R (1999). Expression of matrix metalloproteinase-9 in squamous cell carcinoma of the uterine cervix—clinicopathologic study using immunohistochemistry and mRNA *in situ* hybridization. *Gynecol Oncol* **72**, 380–386.

[31] Haslett C (1992). Resolution of acute inflammation and the role of apoptosis in the tissue fate of granulocytes. *Clin Sci* **83**, 639–648.

[32] Meszaros AJ, Reichner JS, and Albina JE (2000). Macrophage-induced neutrophil apoptosis. *J Immunol* **165**, 435–441.

[33] Li P, Garcia GE, Xia Y, Wu W, Gersch C, Park PW, Truong L, Wilson CB, Johnson R, and Feng L (2005). Blocking of monocytes chemoattractant protein-1 during tubulointerstitial nephritis resulted in delayed neutrophil clearance. *Am J Pathol* **167**, 637–649.

[34] Kuziel WA, Morgan SJ, Dawson TC, Griffin S, Smithies O, Ley K, and Maeda N (1997). Severe reduction in leukocyte adhesion and monocyte extravasation in mice deficient in CC chemokine receptor 2. *Proc Natl Acad Sci USA* **94**, 12053–12058.

[35] Jinnouchi K, Terasaki Y, Fujiyama S, Tomita K, Kuziel WA, Maeda N, Takahashi K, and Takeya M (2003). Impaired hepatic granuloma formation in mice deficient in C-C chemokine receptor 2. *J Pathol* **200**, 406–416.

[36] Wareing MD, Lyon A, Inglis C, Giannoni F, Charo IF, and Sarawar SR (2007). Chemokine regulation of the inflammatory response to a low-dose influenza infection in CCR2$^{-/-}$ mice. *J Leukoc Biol* **81**, 793–801.

[37] Pixley FJ and Stanley ER (2004). CSF-1 regulation of the wandering macrophage: complexity in action. *Trends Cell Biol* **14**, 628–638.

[38] Guleria I and Pollard JW (2001). Aberrant macrophage and neutrophil population dynamics and impaired Th_1 response to *Listeria monocytogenes* in colony-stimulating factor 1–deficient mice. *Infect Immun* **69**, 1795–1807.

[39] Lin EY, Jones JG, Li P, Zhu L, Whitney KD, Muller WJ, and Pollard JW (2003). Progression to malignancy in the polyoma middle T oncoprotein mouse breast cancer model provides a reliable model for human diseases. *Am J Pathol* **163**, 2113–2126.

[40] Wyckoff J, Wang W, Lin EY, Wang Y, Pixley FJ, Stanley ER, Graf T, Pollard JW, Segall J, and Condeelis J (2004). A paracrine loop between tumor cells and macrophages is required for tumor cell migration in mammary tumors. *Cancer Res* **64**, 7022–7029.

[41] Geissmann F, Jung S, and Littman DR (2003). Blood monocytes consist of two principal subsets with distinct migratory properties. *Immunity* **19**, 71–82.

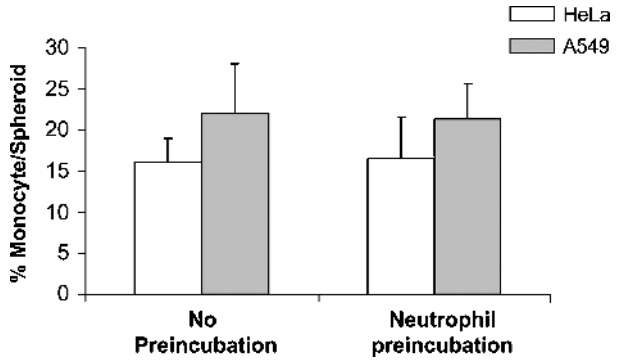

Figure W1. Neutrophils do not inhibit monocyte infiltration into human tumor spheroids *in vitro*. Human tumor (cervical; HeLa or lung; A549) spheroids were cocultured with either monocytes alone for 24 hours or neutrophils for 5 hours followed by monocytes for 24 hours. Flow cytometry of enzymatically dispersed spheroids showed that there were no significant differences ($P = .252$) in the level of monocyte infiltration into spheroids when neutrophils were already present in these structures compared to when they were absent.